

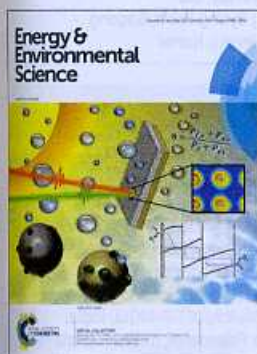
Energy & Environmental Science

www.rsc.org/ees

The Royal Society of Chemistry is the world's leading chemistry community. Through our high impact journals and publications we connect the world with the chemical sciences and invest the profits back into the chemistry community.

IN THIS ISSUE

ISSN 1754-5692 CODEN EESNBY 8(10) 2799-3050 (2015)



Cover
See special collection on Photoelectrochemical Water Splitting, pp. 2809–2901. Image reproduced by permission of Daniel Esposito.



Inside cover
See Antonio Abate *et al.*, pp. 2946–2953. Image reproduced by permission of Felix Freudzon of Freudzon Design International.

EDITORIAL

2809

Photoelectrochemical water splitting

E. L. Miller

The authors in this collection offer comprehensive and definitive summaries of important topics in photoelectrochemical hydrogen production.



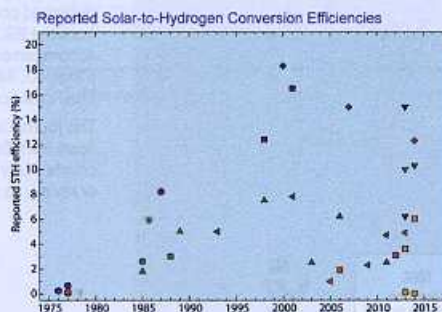
REVIEWS

2811

Experimental demonstrations of spontaneous, solar-driven photoelectrochemical water splitting

Joel W. Ager,* Matthew R. Shaner, Karl A. Walczak, Ian D. Sharp and Shane Ardo

Laboratory demonstrations of spontaneous photoelectrochemical solar water splitting cells are reviewed. Reported solar-to-hydrogen conversion efficiencies are as high as 18%. Reported operational lifetimes are relatively short, with few demonstrations exceeding one week.

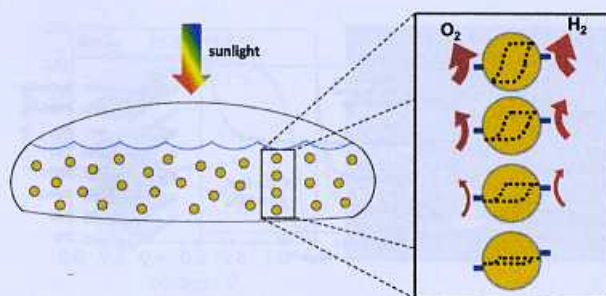


2825

Particle suspension reactors and materials for solar-driven water splitting

David M. Fabian, Shu Hu, Nirala Singh, Frances A. Houle, Takashi Hisatomi, Kazunari Domen, Frank E. Osterloh and Shane Ardo*

Reactor and particle design considerations of particle suspension reactors for solar photoelectrochemical water splitting.

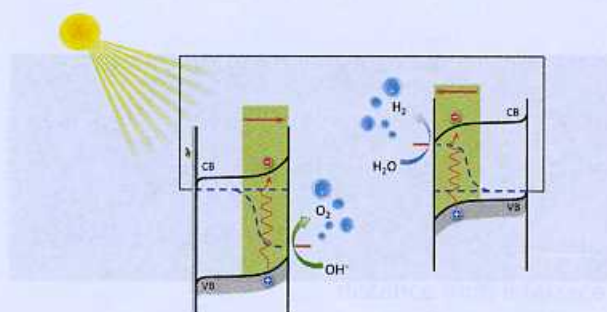


2851

Interfacial band-edge energetics for solar fuels production

Wilson A. Smith,* Ian D. Sharp, Nicholas C. Strandwitz and Juan Bisquert

Theoretical and practical aspects of solid–solid and solid–liquid interfaces for photoelectrochemical (PEC) devices are discussed.

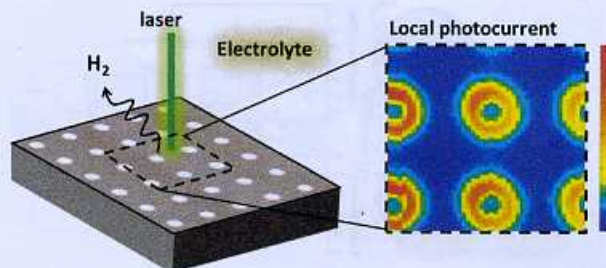


2863

Methods of photoelectrode characterization with high spatial and temporal resolution

Daniel V. Esposito,* Jason B. Baxter, Jimmy John, Nathan S. Lewis, Thomas P. Moffat, Tadashi Ogitsu, Glen D. O'Neil, Tuan Anh Pham, A. Alec Talin, Jesus M. Velazquez and Brandon C. Wood

This article reviews computational and *in situ* experimental tools capable of characterizing the properties and performance of photoelectrodes used for solar fuels production with high spatial and temporal resolution.



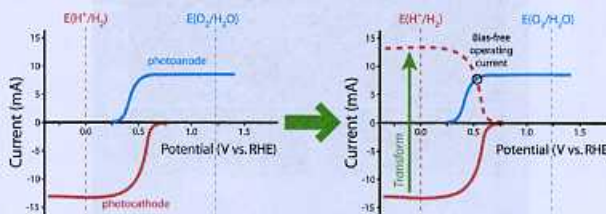
OPINION

2886

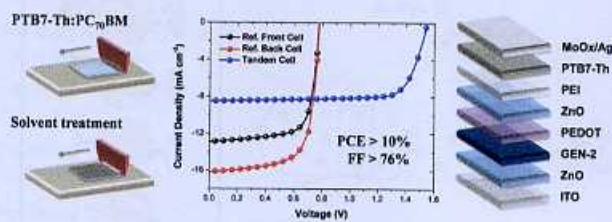
Methods for comparing the performance of energy-conversion systems for use in solar fuels and solar electricity generation

Robert H. Coridan, Adam C. Nielander, Sonja A. Francis, Matthew T. McDowell, Victoria Dix, Shawn M. Chatman and Nathan S. Lewis*

We outline the significance and advantages of different metrics used to characterize photoelectrodes for electrochemical solar energy conversion.



2902

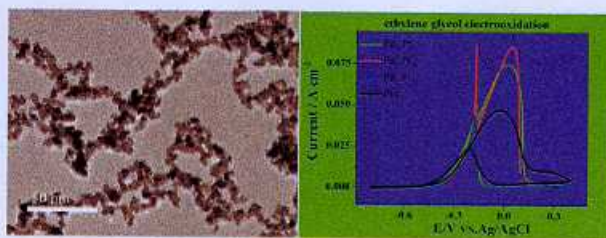


Air-processed polymer tandem solar cells with power conversion efficiency exceeding 10%

Ning Li* and Christoph J. Brabec

Polymer tandem solar cells fabricated by doctor-blading in air achieve a high PCE exceeding 10% along with an unprecedentedly high FF of >76%.

2910

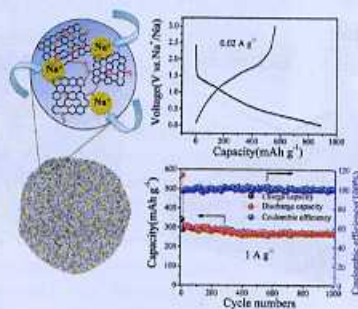


Bimetallic PdPt nanowire networks with enhanced electrocatalytic activity for ethylene glycol and glycerol oxidation

Wei Hong, Changshuai Shang, Jin Wang* and Erkang Wang*

A facile avenue to synthesize bimetallic PdPt nanowire networks with tunable composition and enhanced electrocatalytic performance is demonstrated.

2916

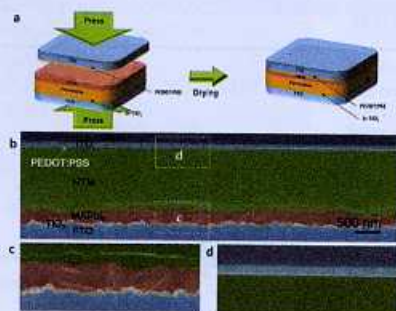


A high performance sulfur-doped disordered carbon anode for sodium ion batteries

Wei Li, Min Zhou, Haomiao Li, Kangli Wang,* Shijie Cheng and Kai Jiang*

Sulfur-doped disordered carbon exhibits high capacity and excellent cyclability as an anode for sodium ion batteries.

2922



Stable semi-transparent $\text{CH}_3\text{NH}_3\text{PbI}_3$ planar sandwich solar cells

Jin Hyuck Heo, Hye Ji Han, Minho Lee, Myungkwan Song, Dong Ho Kim and Sang Hyuk Im*

Semi-transparent MAPbI_3 planar sandwich solar cells were fabricated by simply laminating an F doped tin oxide/ TiO_2 / MAPbI_3 /wet hole transporting material with additives and PEDOT:PSS/indium tin oxide (ITO).

COM

2928

High
thro

J. P. C.
S. Ne
A. R. S
A. Aba
Planar
misali
SnO₂
conver

2935

A gen
defect
from

David
The sta
the nea
perform
applic
where

2941

A zinc
\$100 p

Ke Gor
Jonath
Shuang
A zinc-
cost re
conseq
capital

PAPER

2946

Siloto
hole tr
perovs

Antoni
Juan-P
Taisuke
Klaus H
Moham
Novel h
perovsk

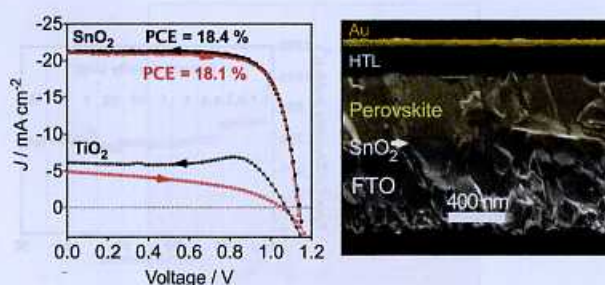
This journal

2928

Highly efficient planar perovskite solar cells through band alignment engineering

J. P. Correa Baena,* L. Steier, W. Tress, M. Saliba, S. Neutzner, T. Matsui, F. Giordano, T. J. Jacobsson, A. R. Srimath Kandada, S. M. Zakeeruddin, A. Petrozza, A. Abate, M. K. Nazeeruddin, M. Grätzel and A. Hagfeldt*

Planar perovskite solar cells exhibit a conduction band misalignment of the perovskite with TiO_2 , but not with SnO_2 . The system using the latter yielded power conversion efficiencies over 18%.

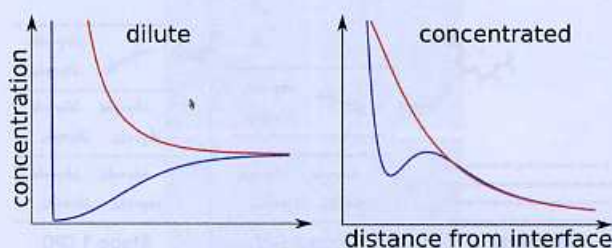


2935

A generalised space-charge theory for extended defects in oxygen-ion conducting electrolytes: from dilute to concentrated solid solutions

David S. Mebane* and Roger A. De Souza

The standard Poisson–Boltzmann approach to modeling the near-interface defect behaviour in solid electrolytes performs well at low dopant concentrations but its applicability is questionable at higher dopant levels where interactions become important.

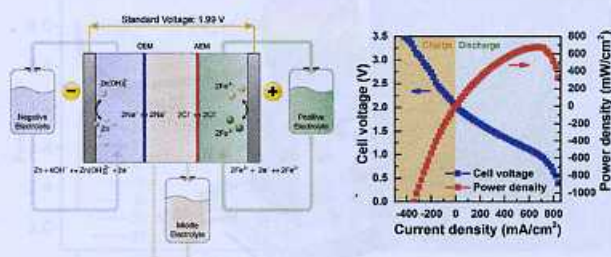


2941

A zinc–iron redox-flow battery under \$100 per kW h of system capital cost

Ke Gong, Xiaoya Ma, Kameron M. Conforti, Kevin J. Kuttler, Jonathan B. Grunewald, Kelsey L. Yeager, Martin Z. Bazant, Shuang Gu* and Yushan Yan*

A zinc–iron redox-flow battery is developed that uses low cost redox materials and delivers high cell performance, consequently achieving an unprecedentedly low system capital cost under \$100 per kW h.



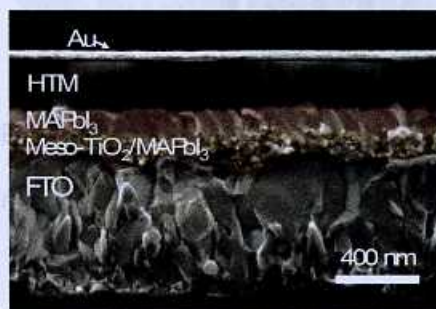
PAPERS

2946

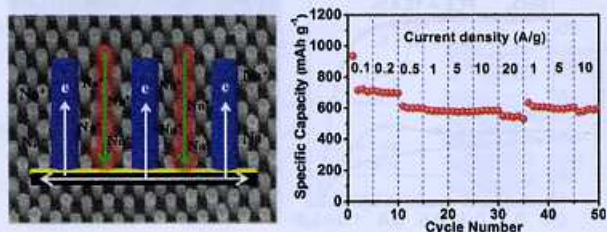
Silolothiophene-linked triphenylamines as stable hole transporting materials for high efficiency perovskite solar cells

Antonio Abate,* Sanghyun Paek, Fabrizio Giordano, Juan-Pablo Correa-Baena, Michael Saliba, Peng Gao, Taisuke Matsui, Jaejung Ko,* Shaik M. Zakeeruddin, Klaus H. Dahmen, Anders Hagfeldt, Michael Grätzel and Mohammad Khaja Nazeeruddin*

Novel hole transporting materials enabled to prepare stable perovskite solar cells.



2954

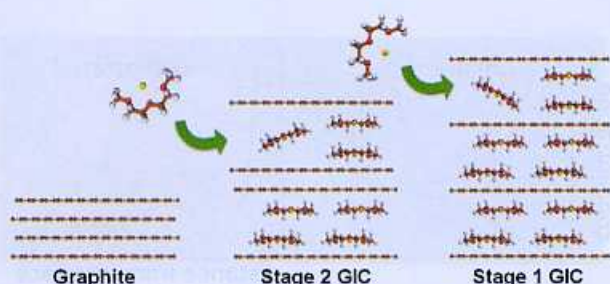


Large-scale highly ordered Sb nanorod array anodes with high capacity and rate capability for sodium-ion batteries

Liyang Liang, Yang Xu, Chengliang Wang, Liaoyong Wen, Yaoguo Fang, Yan Mi, Min Zhou, Huaping Zhao and Yong Lei*

Highly ordered Sb nanorod arrays with large interval spacing were fabricated that showed high capacities and superior rate capabilities.

2963

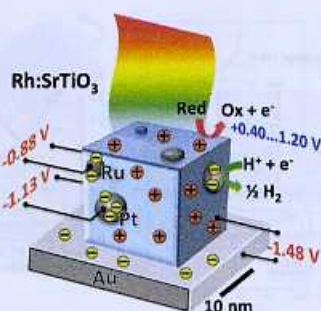


Sodium intercalation chemistry in graphite

Haegyeom Kim, Jihyun Hong, Gabin Yoon, Hunchul Kim, Kyu-Young Park, Min-Sik Park, Won-Sub Yoon and Kisuk Kang*

The solvated-Na-ion intercalation in graphite is investigated in terms of stoichiometry, staging structure, and solvated ion configuration using combined experimental and theoretical studies.

2970

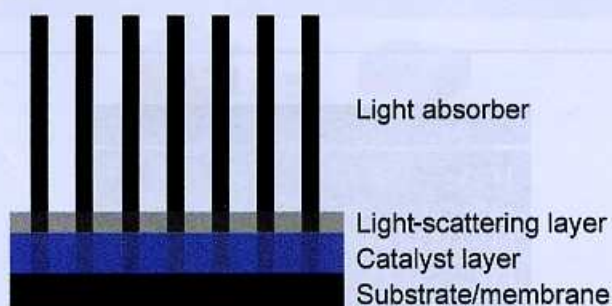


Photochemical charge transfer observed in nanoscale hydrogen evolving photocatalysts using surface photovoltage spectroscopy

J. Wang, J. Zhao and F. E. Osterloh*

The application of inorganic nanostructures for solar water splitting is currently limited by our understanding of photochemical charge transfer on the nanoscale, where space charge layers are less effective for carrier separation.

2977



Functional integration of Ni–Mo electrocatalysts with Si microwire array photocathodes to simultaneously achieve high fill factors and light-limited photocurrent densities for solar-driven hydrogen evolution

Matthew R. Shaner, James R. McKone, Harry B. Gray and Nathan S. Lewis*

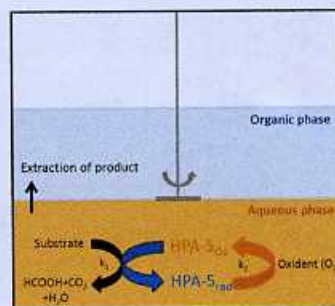
An n⁺p-Si microwire array with a Ni–Mo/TiO₂ catalyst/light-scattering bi-layer structure that simultaneously achieves high fill factors and light-limited photocurrent densities for direct solar H₂(g) production.

2985

Biomass oxidation to formic acid in aqueous media using polyoxometalate catalysts – boosting FA selectivity by *in-situ* extraction

Jenny Reichert, Birgit Brunner, Andreas Jess, Peter Wasserscheid and Jakob Albert*

1-Hexanol and 1-heptanol were applied as *in-situ* extracting agents in the oxidation reaction of biomass to formic acid (FA) using a Keggin-type polyoxometalate (H8PV5Mo7O40) as a homogeneous catalyst, oxygen as the oxidant and water as the solvent.

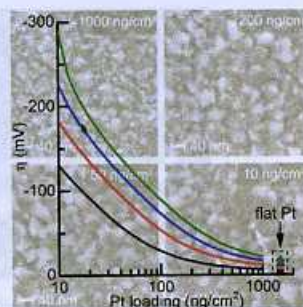


2991

Scalability and feasibility of photoelectrochemical H₂ evolution: the ultimate limit of Pt nanoparticle as an HER catalyst

E. Kemppainen, A. Bodin, B. Sebok, T. Pedersen, B. Seger, B. Mei, D. Bae, P. C. K. Vesborg, J. Halme, O. Hansen, P. D. Lund and I. Chorkendorff*

This study highlights the feasibility to scale-up photoelectrochemical water splitting to the TW level using Pt nanoparticles as hydrogen evolution catalyst.

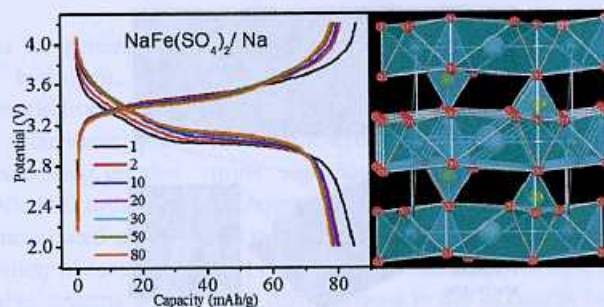


3000

Eldfellite, NaFe(SO₄)₂: an intercalation cathode host for low-cost Na-ion batteries

Preetam Singh, Konda Shiva, Hugo Celio and John B. Goodenough*

The mineral eldfellite, NaFe(SO₄)₂, is characterized as a potential cathode for a Na-ion battery that can be fabricated in charged-state.

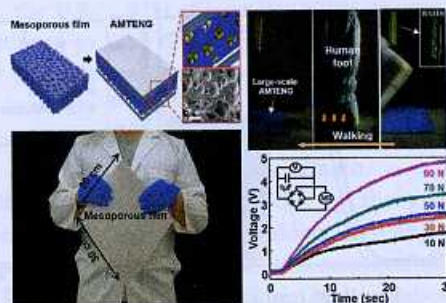


3006

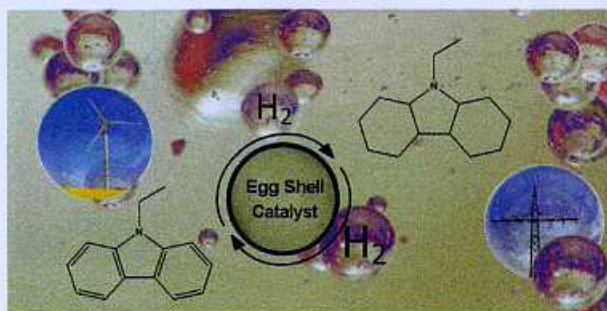
Mesoporous pores impregnated with Au nanoparticles as effective dielectrics for enhancing triboelectric nanogenerator performance in harsh environments

Jinsung Chun, Jin Woong Kim, Woo-suk Jung, Chong-Yun Kang, Sang-Woo Kim, Zhong Lin Wang and Jeong Min Baik*

A facile synthesis of mesoporous films impregnated with Au nanoparticles as effective dielectrics for enhancing the TENG's performance based on vertical contact-separation mode is demonstrated.



3013

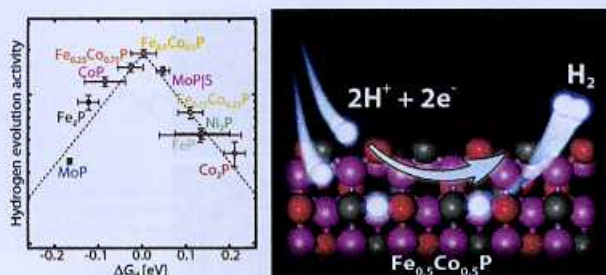


Macrokinetic effects in perhydro-*N*-ethylcarbazole dehydrogenation and H₂ productivity optimization by using egg-shell catalysts

Willi Peters, Alexander Seidel, Stefan Herzog, Andreas Bösmann, Wilhelm Schwieger and Peter Wasserscheid*

This contribution deals with pore diffusion influences on the dehydrogenation kinetics of perhydro-*N*-ethylcarbazole (H12-NEC).

3022

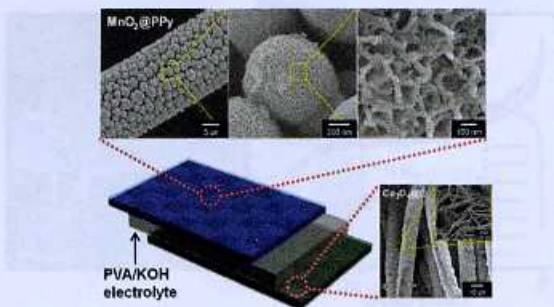


Designing an improved transition metal phosphide catalyst for hydrogen evolution using experimental and theoretical trends

Jakob Kibsgaard, Charlie Tsai, Karen Chan, Jesse D. Benck, Jens K. Nørskov, Frank Abild-Pedersen* and Thomas F. Jaramillo*

A volcano relationship exists between hydrogen evolution activities and hydrogen adsorption free energies for transition metal phosphides. We further predict and confirm that Fe_{0.5}Co_{0.5}P exhibits the highest activity.

3030

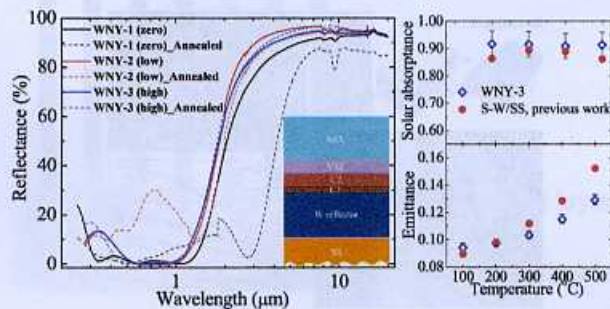


Polypyrrole-coated manganese dioxide with multiscale architectures for ultrahigh capacity energy storage

Jun Seop Lee, Dong Hoon Shin and Jyongsik Jang*

One-dimensional MnO₂-based multiscale micronodules were fabricated through a facile electrodeposition and coating process to produce ultrahigh performance flexible asymmetric supercapacitors.

3040



A high-performance spectrally-selective solar absorber based on a yttria-stabilized zirconia cermet with high-temperature stability

Feng Cao, Daniel Kraemer, Lu Tang, Yang Li, Alexander P. Litvinchuk, Jiming Bao, Gang Chen* and Zhifeng Ren*

We demonstrate a W–Ni–YSZ cermet-based solar absorber with high solar absorptance, low infrared emittance and high thermal stability up to 600 °C.